Cdh1 concentration 0.4 nM) or HeLa cell extract (2 ml)[26] was incubated with 4 μg anti-Cdc27 antibody for 4 h at 4 °C. Immune complexes were captured on protein A Sepharose (Biorad) (50 μl), washed four times in XB buffer (20 mM HEPES pH 7.8, 100 mM KCl, 5 mM $MgCl_2$) supplemented with 1% Triton-X100, washed once with XB buffer with 300 mM NaCl, and once with XB. A total of 5 μl of washed beads were incubated with 1 μl ^{35}S-labelled Skp2, UbCH-10 (2.8 μM) (Boston Biochem), E1 (1 μM) (Boston Biochem) and an ATP-regenerating system[28] in a final volume of 7.5 μl at room temperature with shaking. Ubiquitin (Boston Biochem) or methyl-ubiquitin (Boston Biochem) (10 mg ml^{-1}) was also included, as indicated. Aliquots of 1 μl of the ubiquitination reactions were removed, boiled in SDS-containing sample buffer and resolved by SDS–PAGE.

siRNA

siRNAs were purchased from Dharmacon and transfected into subconfluent cells using Oligofectamine (Invitrogen) according to the manufacturer's instructions. Cdh1 siRNAs were named according to the first Cdh1 codon in their recognition sites and corresponded to Cdh1 nucleotide sequences 266–286 (Cdh1-127), 305–325 (Cdh1-166), 338–358 (Cdh1-199), 566–586 (Cdh1-427) and 602–622 (Cdh1-463). The Cdh1-199 siRNA[29] and Skp2 siRNA[30] were described previously. An siRNA corresponding to a 'scrambled' cyclin A sequence (sense strand 5′-AACAACCUGCCCGCGACGGAA-3′) and a firefly luciferase siRNA served as negative controls.

Pulse–chase analysis

After transfection and synchronization, cells were grown in cysteine/methionine-free media (Invitrogen) for 20 min and labelled in media supplemented with trans-label (50 μl per 100-mm plate, 14 mCi ml^{-1}, ICN) for an additional 20 min. Cells were washed twice with PBS and chased with DMEM supplemented with 10% fetal bovine serum, 2 mM cysteine and 2 mM methionine. At various time points thereafter cell extracts were prepared in PBS containing 1% Triton-X100 and incubated with anti-HA antibody coupled to protein A sepharose (Santa Cruz) for 24 h at 4 °C. Immunoprecipitates were washed four times in PBS 1% Triton-X100, once in RIPA buffer, and analysed by SDS–PAGE.

Received 24 November 2003; accepted 27 January 2004; doi:10.1038/nature02381.

1. Nakayama, K. I., Hatakeyama, S. & Nakayama, K. Regulation of the cell cycle at the G1–S transition by proteolysis of cyclin E and p27Kip1. *Biochem. Biophys. Res. Commun.* **282,** 853–860 (2001).
2. Peters, J. M. The anaphase-promoting complex. Proteolysis in mitosis and beyond. *Mol. Cell* **9,** 931–943 (2002).
3. Harper, J. W., Burton, J. L. & Solomon, M. J. The anaphase-promoting complex: it's not just for mitosis any more. *Genes Dev.* **16,** 2179–2206 (2002).
4. Zhang, H., Kobayashi, R., Galaktionov, K. & Beach, D. p19Skp1 and p45Skp2 are essential elements of the cyclin A-CDK2 S phase kinase. *Cell* **82,** 915–925 (1995).
5. Imaki, H. *et al.* Cell cycle-dependent regulation of the Skp2 promoter by GA-binding protein. *Cancer Res.* **63,** 4607–4613 (2003).
6. Wirbelauer, C. *et al.* The F-box protein Skp2 is a ubiquitylation target of a Cul1-based core ubiquitin ligase complex: evidence for a role of Cul1 in the suppression of Skp2 expression in quiescent fibroblasts. *EMBO J.* **19,** 5362–5375 (2000).
7. Zachariae, W. & Nasmyth, K. Whose end is destruction: cell division and the anaphase-promoting complex. *Genes Dev.* **13,** 2039–2058 (1999).
8. Schwab, M., Neutzner, M., Mocker, D. & Seufert, W. Yeast Hct1 recognizes the mitotic cyclin Clb2 and other substrates of the ubiquitin ligase APC. *EMBO J.* **20,** 5165–5175 (2001).
9. McGarry, T. J. & Kirschner, M. W. Geminin, an inhibitor of DNA replication, is degraded during mitosis. *Cell* **93,** 1043–1053 (1998).
10. Fang, G., Yu, H. & Kirschner, M. W. Direct binding of CDC20 protein family members activates the anaphase-promoting complex in mitosis and G1. *Mol. Cell* **2,** 163–171 (1998).
11. Pfleger, C. M., Lee, E. & Kirschner, M. W. Substrate recognition by the Cdc20 and Cdh1 components of the anaphase-promoting complex. *Genes Dev.* **15,** 2396–2407 (2001).
12. Sorensen, C. S. *et al.* Nonperiodic activity of the human anaphase-promoting complex-Cdh1 ubiquitin ligase results in continuous DNA synthesis uncoupled from mitosis. *Mol. Cell. Biol.* **20,** 7613–7623 (2000).
13. Nakayama, K. *et al.* Targeted disruption of Skp2 results in accumulation of cyclin E and p27(Kip1), polyploidy and centrosome overduplication. *EMBO J.* **19,** 2069–2081 (2000).
14. von der Lehr, N. *et al.* The F-box protein Skp2 participates in c-Myc proteasomal degradation and acts as a cofactor for c-Myc-regulated transcription. *Mol. Cell* **11,** 1189–1200 (2003).
15. Kim, S. Y., Herbst, A., Tworkowski, K. A., Salghetti, S. E. & Tansey, W. P. Skp2 regulates Myc protein stability and activity. *Mol. Cell* **11,** 1177–1188 (2003).
16. Sutterluty, H. *et al.* p45SKP2 promotes p27Kip1 degradation and induces S phase in quiescent cells. *Nature Cell Biol.* **1,** 207–214 (1999).
17. Latres, E. *et al.* Role of the F-box protein Skp2 in lymphomagenesis. *Proc. Natl Acad. Sci. USA* **98,** 2515–2520 (2001).
18. Nelsen, C. J. *et al.* Induction of hepatocyte proliferation and liver hyperplasia by the targeted expression of cyclin E and skp2. *Oncogene* **20,** 1825–1831 (2001).
19. Gstaiger, M. *et al.* Skp2 is oncogenic and overexpressed in human cancers. *Proc. Natl Acad. Sci. USA* **98,** 5043–5048 (2001).
20. Bloom, J. & Pagano, M. Deregulated degradation of the cdk inhibitor p27 and malignant transformation. *Semin. Cancer Biol.* **13,** 41–47 (2003).
21. Bashir, T., Dorrello, N., Amador, V., Guardavaccaro, D. & Pagano, M. Control of the $SCF^{Skp2\text{-}Cks1}$ ubiquitin ligase by the APC/C^{Cdh1} ubiquitin ligase. *Nature* **428,** 190–193 (2004).
22. Murray, A. W. & Kirschner, M. W. Dominoes and clocks: the union of two views of the cell cycle. *Science* **246,** 614–621 (1989).
23. Ayad, N. G. *et al.* Tome-1, a trigger of mitotic entry, is degraded during G1 via the APC. *Cell* **113,** 101–113 (2003).
24. Sorensen, C. S. *et al.* A conserved cyclin-binding domain determines functional interplay between anaphase-promoting complex-Cdh1 and cyclin A-Cdk2 during cell cycle progression. *Mol. Cell. Biol.* **21,** 3692–3703 (2001).
25. Kaelin, W. G., Pallas, D. C., DeCaprio, J. A., Kaye, F. J. & Livingston, D. M. Identification of cellular proteins that can interact specifically with the T/E1A-binding region of the retinoblastoma gene product. *Cell* **64,** 521–532 (1991).
26. Wan, Y., Liu, X. & Kirschner, M. W. The anaphase-promoting complex mediates TGF-β signaling by targeting SnoN for destruction. *Mol. Cell* **8,** 1027–1039 (2001).
27. Pfleger, C. M. & Kirschner, M. W. The KEN box: an APC recognition signal distinct from the D box targeted by Cdh1. *Genes Dev.* **14,** 655–665 (2000).
28. Murray, A. Cell cycle extracts. *Methods Cell Biol.* **36,** 581–605 (1991).
29. Brummelkamp, T. R., Bernards, R. & Agami, R. A system for stable expression of short interfering RNAs in mammalian cells. *Science* **296,** 550–553 (2002).
30. Mendez, J. *et al.* Human origin recognition complex large subunit is degraded by ubiquitin-mediated proteolysis after initiation of DNA replication. *Mol. Cell* **9,** 481–491 (2002).

Supplementary Information accompanies the paper on **www.nature.com/nature**.

Acknowledgements We thank W. Harper, J. Lukas and M. Meyerson for critical reading of the manuscript; J. Lukas for reagents; M. Pagano for sharing unpublished data; and members of the Kirschner and Kaelin Laboratories for useful discussions. W.G.K. is a Howard Hughes Medical Institute Investigator. This work is supported in part by NIH grants to M.W.K. and W.G.K.

Competing interests statement The authors declare that they have no competing financial interests.

Correspondence and requests for materials should be addressed to M.W.K. (marc@hms.harvard.edu) or W.G.K. (william_kaelin@dfci.harvard.edu).

Insight into tubulin regulation from a complex with colchicine and a stathmin-like domain

Raimond B.G. Ravelli[1]*, Benoît Gigant[2]*, Patrick A. Curmi[3], Isabelle Jourdain[3], Sylvie Lachkar[3], André Sobel[3] & Marcel Knossow[2]

[1]*European Molecular Biology Laboratory (EMBL), Grenoble Outstation, 6 rue Jules Horowitz, BP 181, 38042 Grenoble Cedex 9, France*
[2]*Laboratoire d'Enzymologie et Biochimie Structurales, UPR 9063, Centre National de la Recherche Scientifique, Bâtiment 34, 1 avenue de la Terrasse, 91198 Gif-sur-Yvette Cedex, France*
[3]*U440 INSERM/UPMC, Institut du Fer à Moulin, 17 rue du Fer à Moulin, 75005 Paris, France*

* These authors contributed equally to this work

Microtubules are cytoskeletal polymers of tubulin involved in many cellular functions. Their dynamic instability is controlled by numerous compounds and proteins, including colchicine[1] and stathmin family proteins[2,3]. The way in which microtubule instability is regulated at the molecular level has remained elusive, mainly because of the lack of appropriate structural data. Here, we present the structure, at 3.5 Å resolution, of tubulin in complex with colchicine and with the stathmin-like domain (SLD) of RB3. It shows the interaction of RB3-SLD with two tubulin heterodimers in a curved complex capped by the SLD amino-terminal domain, which prevents the incorporation of the complexed tubulin into microtubules. A comparison with the structure of tubulin in protofilaments[4] shows changes in the subunits of tubulin as it switches from its straight conformation to a curved one. These changes correlate with the loss of lateral contacts and provide a rationale for the rapid microtubule depolymerization characteristic of dynamic instability. Moreover, the tubulin–colchicine complex sheds light on the mechanism of colchicine's activity: we show that colchicine binds at a location where it prevents curved tubulin from adopting a straight structure, which inhibits assembly.

Tubulin, an αβ heterodimer initially identified as the cellular colchicine-binding protein[5,6], is the target of numerous small-molecule ligands that interfere with microtubule dynamics, several

of which are of clinical use, in particular for cancer treatment. Most of them bind to one of three different sites: the colchicine, vinblastine and taxol sites. Whereas the taxol site has been identified in the structure of tubulin protofilaments in Zn-sheets[4], the locations of the other two sites are still uncertain (see, for example, ref. 7). Tubulin also interacts with regulatory cellular proteins, among which stathmin[2,8], or each SLD of its related vertebrate proteins, sequesters two tubulin heterodimers[3,9,10].

We previously reported a partial structure of the tubulin:RB3-SLD complex (T2R)[11], determined on the basis of the structure of the tubulin heterodimer in Zn-sheets. This defined the complex as a head-to-tail assembly of two tubulin molecules whose curvature is maintained by a long RB3-SLD α-helix modelled as a ~90-residue poly-Ala α-helix whose direction could not be assigned. The current tubulin–colchicine:RB3-SLD complex structure has been determined at higher resolution using experimental phases to avoid model bias[12]. It allows us (1) to trace and refine the RB3-SLD polypeptide chain in interaction with tubulin along nearly its entire length, (2) to rebuild tubulin heterodimers and compare their structures in a curved, soluble assembly and in protofilaments and (3) to define the interactions of tubulin with colchicine.

In the complex, RB3-SLD adopts a hook-like shape accommodating the two bound tubulin heterodimers (Fig. 1a). RB3-SLD comprises three domains: an N-terminal 'cap' domain (residues 4 to 28) that is conserved in the stathmin family, a variable linker domain (residues 29 to 45) and a conserved, mostly α-helical carboxy-terminal domain (residues 46 to 145)[13]. Within the N-terminal cap domain, residues 7 to 23 form a β-hairpin (Fig. 1b) that extends the β-sheet of the intermediate domain[4] of the α-tubulin subunit located at one end of the T2R complex. This extension, together with nearby interactions (Fig. 1c), contributes significantly to the stability of the tubulin–colchicine:RB3-SLD complex. Interestingly, Ser 16, which is conserved in the stathmin family and phosphorylated in stathmin in response to a number of signals[14], is located in the tight turn of the β-hairpin (Fig. 1c) and its phosphorylation could inhibit proper formation of the N-terminal cap structure. Furthermore, the residues of tubulin interacting with the N-terminal cap mediate longitudinal contacts between tubulin heterodimers assembled in protofilaments[15]. The SLD would therefore sterically hinder the incorporation of the T2R complex at the (+)-end of microtubules via its N-terminal cap (Fig. 1b), in addition to maintaining the curvature via its C-terminal helix[11]. The capping interaction also explains why RB3-SLD (data not shown) and stathmin, but not an N-terminally truncated form, prevent the formation of tubulin rings[9,16]. The SLD linker domain involves a proline-rich region that diverges most among SLDs in the stathmin family[3,13]. This region has no regular secondary structure and is the least ordered part of RB3-SLD in the complex.

Finally, in the RB3-SLD C-terminal domain, electron density for the largest side chains together with three selenomethionine markers permitted the unambiguous assignment of the helical register. In the structure, the majority of the side-chains that

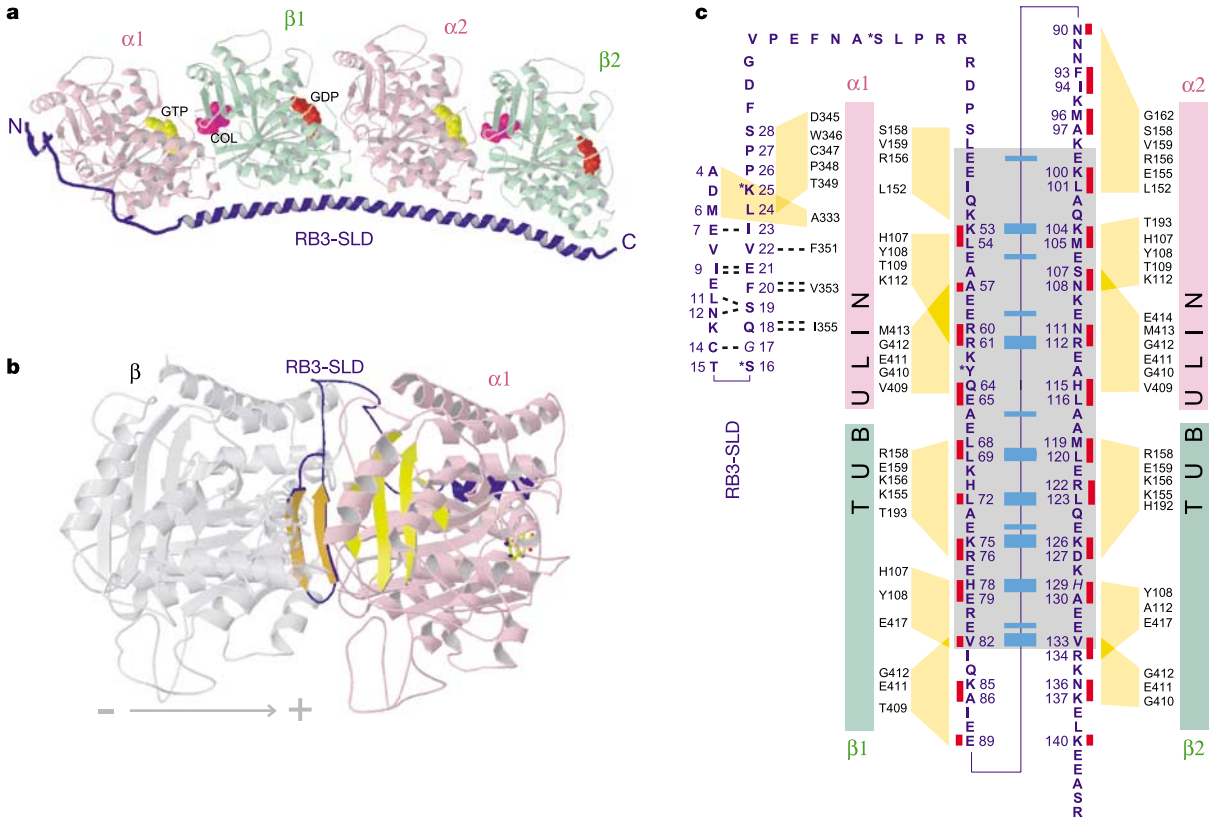

Figure 1 The tubulin–colchicine:RB3-SLD complex. **a**, The complex includes two tubulin αβ heterodimers, with colchicine bound to β subunits at the interface with α. The RB3-SLD connecting region (residues 29–45) is from tubulin–podophyllotoxin:RB3-SLD, where it is clearest (podophyllotoxin is a competitive inhibitor of colchicine binding to tubulin[23]). **b**, The β hairpin (orange) in the N-terminal domain of RB3-SLD caps the T2R complex, extending the β sheet (yellow) of the intermediate domain in the α1 subunit. The extensive overlap with a protofilament (+)-end β subunit[15], preventing the addition of the T2R complex to a microtubule, is illustrated. **c**, Interactions of RB3-SLD residues with tubulin (except for the least-well-defined RB3-SLD connecting region and for the extension of the tubulin intermediate domain β-sheet) represented by yellow connecting areas. Red bars, residues of the α-helix pointing towards tubulin. Dashed lines, main-chain hydrogen bonds in the extension of the intermediate domain β-sheet. Within the internal repeat (grey), identical residues are connected in blue (thick blue, side-chain pointing towards tubulin). Asterisks indicate positions of stathmin phosphorylation sites.

point towards tubulin are defined and most of the previously proposed tubulin residues that interact with stathmin are confirmed[11] (Fig. 1c). The interacting SLD residues include the residues of the mostly hydrophobic seam proposed to be responsible for the interaction[17], but also at least as many polar/charged residues. The data also show that, as hypothesized previously[11], each sequence of the repeated pair present in the C-terminal α-helix is identically positioned relative to the corresponding tubulin heterodimer. Remarkably, side chains of six of the 13 repeated residue pairs point away from tubulin (Fig. 1c), raising the possibility of a function of the duplicated sequence and these conserved residues in addition to tubulin binding.

A comparison of the structure of tubulin heterodimers in T2R (which is similar to that of GDP–tubulin in curved protofilaments[11]) and in straight protofilaments demonstrates three important differences. First, a rotation of 11.6° ± 1.0° is required to superimpose their α and β subunits in the T2R complex. This is not affected by the presence of colchicine, because this rotation was unchanged in lower-resolution diffracting crystals that did not include colchicine.

Second, the relative orientation of the three tubulin subunit domains[18]—the N-terminal nucleotide-binding domain, the intermediate domain and the C-terminal domain made of two antiparallel α-helices—is different. The nucleotide-binding and C-terminal domains of each subunit form a rigid block: the root-mean-square deviation (r.m.s.d.) of Cα positions in secondary structure elements of these domains in the curved (this work) and straight[4] structures is 0.9 Å. In both α and β, however, an 8° and 11° rotation, respectively, of their intermediate domains is required to superimpose them in the two structures (the r.m.s.d. of the positions of Cα atoms in secondary structure elements after superposition is 0.8 Å) (Fig. 2a).

Third, there are noticeable local differences between the curved and straight structures. They comprise conformational changes in loops located at longitudinal interfaces in protofilaments[15] and also changes in the long, flexible, M and H1–S2 loops, mostly due to the influence of crystal packing (for the nomenclature of tubulin secondary structure elements and loops, see ref. 4). Changes at the intradimer α–β interface comprise a movement of the β subunit T7 loop and H8 helix, which lie close to the colchicine-binding site (the r.m.s.d. of Cα positions after superimposition of the β subunit intermediate domains is 4.9 Å, maximum deviation is 6.6 Å), as well as differences in the conformations of the α subunit T5 and H6–H7 loops. The latter accompanies a 1.5 Å translation of the H7 helix along its axis. Changes between the curved and straight structures at the interdimer α–β interface are even more extensive, with two major differences, both in the β subunit: a different T5 loop conformation and a movement in one block of the H6–H7 loop following a 2.5 Å translation of the H7 helix along its axis, dragging along the C-terminal end of helix H6. In the conformation they adopt in the curved T2R structure, the T5 and H6–H7 loops of a subunit would interfere with the neighbouring subunit positioned as across a longitudinal straight protofilament interface (Fig. 2b; Supplementary Fig. 1).

The T5 and H6–H7 loops contribute to the establishment of a kinetic barrier between tubulin straight and curved structures, because they switch between two conformations when this transition happens. The unfavourable interactions of the H6–H7 loop that prevent the straight assembly of tubulin heterodimers will be observed unless the H7 helix switches back to its location in the straight structure. This helix connects the nucleotide-binding and intermediate domains; in both the α and β subunits and in the curved and straight structures, residues in its C-terminal half contact β-strands S7, S8 and S10 of the intermediate domain. As a consequence, for the H7 helix to occupy its location in the straight structure, the intermediate domain will rotate towards the nucleotide-binding domain (Fig. 2c). This rotation allows the tubulin structure in microtubules to be stabilized through lateral interactions mediated in the intermediate domain by the M loop and, to a smaller extent, by the H9 and H10 helices[19].

The movements described here do not directly or solely depend on GTP hydrolysis because they occur both in GTP-bound

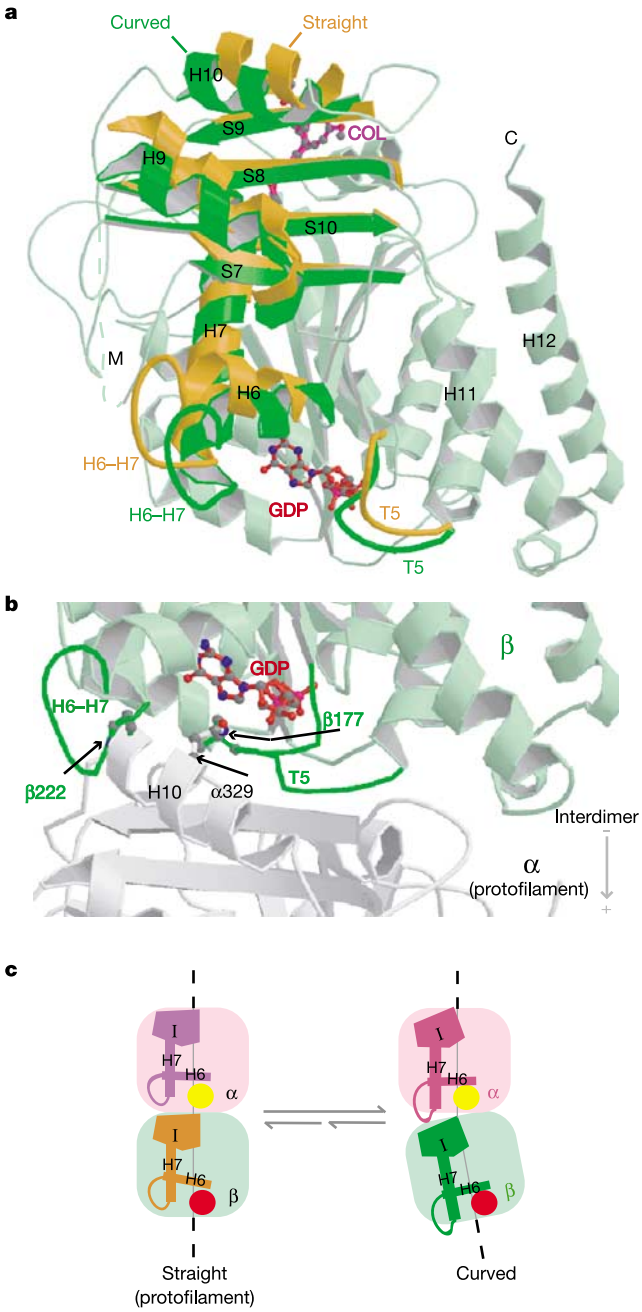

Figure 2 Tubulin subunit changes between the curved and straight structures. **a**, The N-terminal nucleotide-binding and C-terminal domains of β subunits in T2R and protofilaments are superimposable. Changes in the intermediate domains secondary structure elements, the H6–H7 helices as well as the T5 and H6–H7 loops (bright colours) in T2R (green) and protofilaments (orange) are shown. Poorly defined M-loop residues that were not traced are presented as a dashed line. **b**, The interference between a T2R β subunit and a protofilament α subunit positioned as across an interdimer longitudinal interface. For clarity only two β subunit residues, β222 and β177, which would make strongly disfavoured interactions with helix H10 of the α subunit (with the main-chain and residue α329, respectively), are presented. **c**, Cartoon representing the displacement of the intermediate domain (I) in α and β during their curved-to-straight conformation switches.

α subunits and GDP-bound β subunits. The coupling of unfavourable longitudinal interactions to the movement of the intermediate domain suggests a reciprocal link between straight tubulin assembly and lateral interactions: lateral interactions force the straight tubulin conformation to be adopted and allow microtubules to assemble and, reciprocally, straight tubulin assembly allows lateral interactions to be established all along microtubule protofilaments.

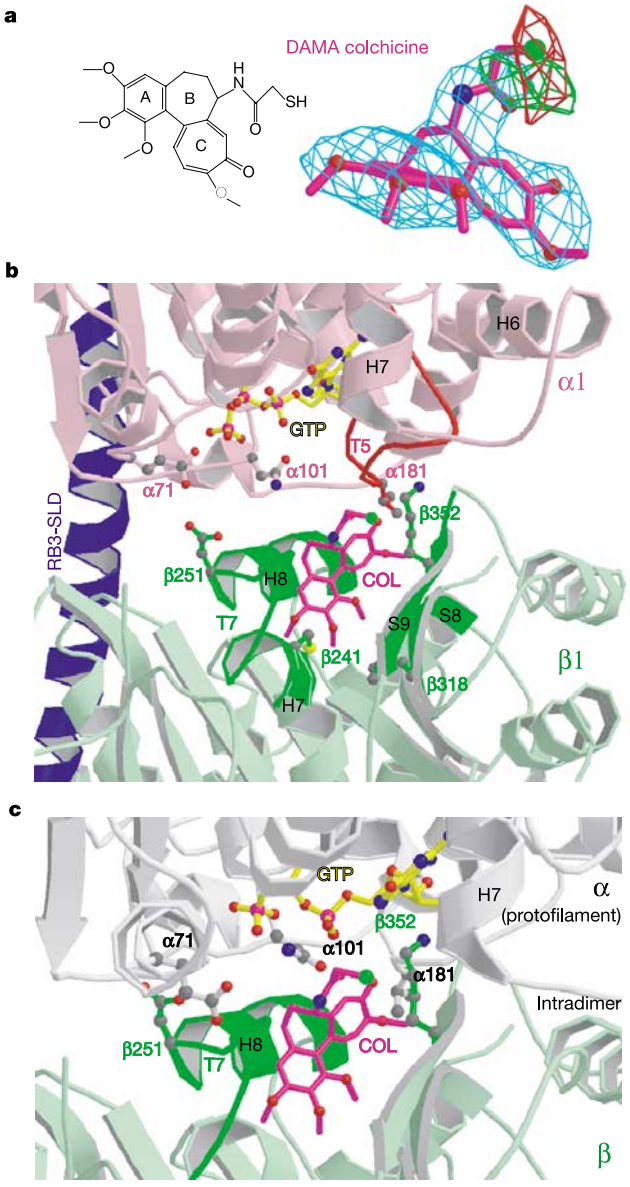

Figure 3 The colchicine-binding site on tubulin. **a**, DAMA-colchicine superimposed on electron-density maps. The 3.5 Å F_{obs}–F_{calc} omit map (cyan) is contoured at 3σ. The 4 Å F_{obs}–F_{calc} maps calculated with colchicine (red, contoured at 3σ) and with DAMA-colchicine but F_{obs} of a tubulin–colchicine:RB3-SLD complex (green, contoured at −3.3σ) are also presented. **b**, The colchicine site in the tubulin–colchicine:RB3-SLD complex (bright colours: tubulin loops and secondary structure elements contacting colchicine). **c**, Interference between colchicine binding and the straight conformation of tubulin in protofilaments. An α subunit is positioned near a colchicine-bound β subunit as across an intradimer longitudinal contact in a protofilament. The α-tubulin subunit is prevented from occupying this position because of: (1) steric hindrance between colchicine and residues α101, α181 and GTP; and (2) colchicine forcing the T7 loop, H8 helix (for clarity, only side chains of two interfering residues—α71 and β251—are presented) and the Lys β352 side chain to interfere with α-tubulin.

Our observations also suggest that, in addition to a loss of lateral interaction energy, depolymerization of one protofilament induces a destabilization of the neighbouring one whose intermediate domains it contacts, by letting it curve. Indeed, curvature causes additional losses of lateral (see above) and of longitudinal interaction energy, as longitudinal interactions are much less extensive in curved structures than in microtubules (the longitudinal interface areas are 1,960 Å^2 and 2,200 Å^2 in T2R compared with 3,000 Å^2 in straight protofilaments[15]). This will lead to easier onset of microtubule disassembly and to enhanced depolymerization speed of GDP–tubulin, two essential features of dynamic instability.

An unresolved issue is the structural mechanism by which GTP regulates microtubule dynamics. One possibility is that binding of GTP to the tubulin β subunit results in a conformational change that locks the H7 lever helix[20] in its straight tubulin structure position through interactions at its N-terminal end. This would be propagated to the α–β interface and possibly to the α subunit owing to an induced movement of the intermediate domain, 'winding up' the tubulin heterodimer into a straighter[21] or ready-to-be-straightened conformation. In microtubules, lateral interactions would then double-lock the H7 helix through contacts at its C-terminal end with the intermediate domain, as described above. Following GTP hydrolysis, the first lock would be loosened; the tubulin heterodimer would then be maintained in its straight structure thanks to lateral interactions, but ready to curve and disassemble in an auto-catalytic process as soon as these interactions are lost.

The colchicine-binding site in tubulin (Fig. 3) was identified during refinement by inspection of the σ_a-weighted[22] F_{obs}–F_{calc} electron-density difference maps (highest peak height, colchicine, is 12 σ; first peak at a different location is 6 σ). There is one such site on each tubulin heterodimer. We also determined the 4.2 Å structure of a ternary tubulin–podophyllotoxin:RB3-SLD complex and found that podophyllotoxin binds to tubulin at the same site as colchicine (Supplementary Fig. 2), consistent with its ability to compete with colchicine binding[23]. A complex where colchicine was replaced by *N*-deacetyl-*N*-(2-mercaptoacetyl)-colchicine (DAMA-colchicine) allowed us to establish the location of the *N*-acetyl group and to define unambiguously the colchicine orientation in its asymmetric electron density (Fig. 3a). The colchicine site is mostly buried in the intermediate domain of the β subunit, boxed in by strands S8 and S9, loop T7 and helices H7 and H8. Colchicine also interacts with loop T5 of the neighbouring α subunit (Fig. 3b), consistent with the observation that colchicine stabilizes the tubulin heterodimer[24].

The structure correlates well with biochemical data showing that β318 tubulin variants have a reduced sensitivity to colchicine[25], and that colchicine derivatives substituted at the methoxy positions of ring A can be crosslinked with Cys β241 (ref. 7). These studies were performed in the absence of any SLD, so the location of colchicine in the tubulin:RB3-SLD complex is expected to be very similar to that in tubulin. It is interesting to note that there is a movement of the T7 loop and of the H8 helix in the tubulin–colchicine complex compared with protofilament tubulin, which makes space available for colchicine binding. This movement is one reason that the observed colchicine site differs from previously proposed sites modelled on the basis of the protofilament structure of tubulin[7].

The effect of colchicine on microtubules has been studied *in vitro* using the preformed tubulin–colchicine complex, which incorporates at the end of microtubules[26]. At a low concentration of tubulin–colchicine, microtubule growth is hindered and microtubule dynamics is inhibited, whereas at high concentration microtubules depolymerize[1]. What is the structural basis for these effects? Microtubule stability requires both longitudinal and lateral interactions between tubulin molecules; the M loops of straight tubulin subunits are the central elements of the latter interactions[15]. When tubulin–colchicine is added to a microtubule, the lateral contacts of the subunit at the newly formed end of the protofilament are not

established because the M loop is displaced (by more than 9 Å in the structure). This is because the straight tubulin conformation is not adopted, as it would lead to a steric clash of colchicine with the α subunit (Fig. 3c). The microtubule mass will stay preserved as long as the proportion of missing lateral contacts remains small. This will be the case at low concentrations of added tubulin–colchicine, as observed[1]. By contrast, at high tubulin–colchicine concentrations, as the proportion of missing lateral contacts increases, destabilized microtubule ends will lead to disassembly.

In conclusion, our data establish a relationship between the onset and speed of microtubule disassembly and the changes in tubulin subunits when tubulin switches from its straight to its curved conformation. They further provide a molecular description of the interaction of RB3-SLD and colchicine with tubulin. We expect that our results will be useful also for the development of novel therapeutic colchicinoid analogues. □

Methods

Protein purification and crystallization

See Supplementary Information.

Data collection and structure determination

The crystals often cracked upon soaking and were radiation sensitive, so hundreds had to be screened for isomorphous pieces suitable for data collection under cryogenic conditions. All data were collected on ID14-4 at the European Synchrotron Radiation Facility (ESRF). Despite the relatively weak diffraction power of the crystals, excellent data could be obtained, especially at low resolution (10–6 Å). In contrast to several other structures of large complexes, we have chosen a strategy to minimize the presence of heavy atoms and carefully examined the decay of anomalous signals during data collection. Where possible, data were corrected for radiation damage[27].

Experimental phases were obtained using a 3.5 Å native data set, a 4.0 Å SeMet SAD (single-wavelength anomalous dispersion) data set collected at 15 K, a 3.8 Å PIP SAD data set and a 4.5 Å Yb MAD (multiple-wavelength anomalous dispersion) data set. Data set statistics are given in Supplementary Table 1. The program SHARP[28] was used for phasing, aided by an iteration of phasing and model refinement, using model phases as external phases in the refinement of the heavy atom sites. The asymmetric unit contains two tubulin heterodimers and one molecule of RB3-SLD. The experimental phases were further improved by density-averaging the two α- and two β-tubulin subunits separately, using the program DM[22]. The resulting 3.5 Å experimental map is of excellent quality (Supplementary Fig. 3) and reveals many side chains after sharpening by applying a resolution-dependent factor $\exp(-Bd^2)$, where d is the resolution and $B = -50\ \text{Å}^2$ (ref. 22).

Model building and refinement

The register of the RB3-SLD sequence and electron density was unambiguously determined using the SeMet sites as anchors and verified by the presence of density of larger side chains such as Tyr 63, His 78 and His 129. The program REFMAC[22,29] was used for restrained positional refinement with a maximum-likelihood target function including experimental phase information. About 5% of the residues are currently modelled as alanines. The two α and two β subunits were restrained separately by non-crystallographic symmetry. The R-factor (R_{free}) is 23% (25%) for all reflections between 20 and 3.5 Å and $I/\sigma_I > -3$. An example of the final map is in Supplementary Fig. 1b. The position of the sulphur atom in DAMA-colchicine was ascertained by refining a model with DAMA-colchicine using diffraction data from a complex containing colchicine and locating a negative peak in the F_{obs}–F_{calc} map close to the location of the sulphur atom (Fig. 3a).

Structure analysis

The angle of the rotation that superimposes tubulin subunits in the T2R complex was determined by least squares using coordinates of tubulin:RB3-SLD complexes determined from independently collected diffraction data sets. The value given is the average of 20 determinations, using ten data sets. The largest conformationally invariant fragment in tubulin subunits when comparing the straight and curved structures was identified using a genetic algorithm[30].

Received 12 December 2003; accepted 4 February 2004; doi:10.1038/nature02393.

1. Panda, D., Daijo, J. E., Jordan, M. A. & Wilson, L. Kinetic stabilization of microtubule dynamics at steady state *in vitro* by substoichiometric concentrations of tubulin-colchicine complex. *Biochemistry* **34,** 9921–9929 (1995).
2. Belmont, L. D. & Mitchison, T. J. Identification of a protein that interacts with tubulin dimers and increases the catastrophe rate of microtubules. *Cell* **84,** 623–631 (1996).
3. Charbaut, E. *et al.* Stathmin family proteins display specific molecular and tubulin binding properties. *J. Biol. Chem.* **276,** 16146–16154 (2001).
4. Löwe, J., Li, H., Downing, K. H. & Nogales, E. Refined structure of αβ-tubulin at 3.5 Å resolution. *J. Mol. Biol.* **313,** 1045–1057 (2001).
5. Weisenberg, R. C., Borisy, G. G. & Taylor, E. W. The colchicine-binding protein of mammalian brain and its relation to microtubules. *Biochemistry* **7,** 4466–4479 (1968).
6. Bane Hastie, S. Interactions of colchicine with tubulin. *Pharmacol Ther.* **51,** 377–401 (1991).
7. Bai, R. *et al.* Mapping the binding site of colchicinoids on β-tubulin. *J. Biol. Chem.* **275,** 40443–40452 (2000).
8. Cassimeris, L. The oncoprotein 18/stathmin family of microtubule destabilizers. *Curr. Opin. Cell Biol.* **14,** 18–24 (2002).
9. Jourdain, L., Curmi, P., Sobel, A., Pantaloni, D. & Carlier, M.-F. Stathmin is a tubulin sequestering protein which forms a ternary T2S complex with two tubulin molecules. *Biochemistry* **36,** 10817–10821 (1997).
10. Curmi, P. A. *et al.* The stathmin tubulin interaction *in vitro*. *J. Biol. Chem.* **272,** 25029–25036 (1997).
11. Gigant, B. *et al.* The 4 Å X-ray structure of a tubulin:stathmin-like domain complex. *Cell* **102,** 809–816 (2000).
12. Burling, F. T., Weis, W. I., Flaherty, K. M. & Brunger, A. T. Direct observation of protein solvation and discrete disorder with experimental crystallographic phases. *Science* **271,** 72–77 (1996).
13. Maucuer, A., Moreau, J., Mechali, M. & Sobel, A. Stathmin gene family: phylogenetic conservation and developmental regulation in *Xenopus*. *J. Biol. Chem.* **268,** 16420–16429 (1993).
14. Beretta, L., Dobransky, T. & Sobel, A. Multiple phosphorylation of stathmin: identification of four sites phosphorylated in intact cells and *in vitro* by cyclic-AMP dependent protein kinase and p34cdc2. *J. Biol. Chem.* **268,** 20076–20084 (1993).
15. Nogales, E., Whittaker, M., Milligan, R. A. & Downing, K. H. High-resolution model of the microtubule. *Cell* **96,** 79–88 (1999).
16. Steinmetz, M. O. *et al.* Op18/stathmin caps a kinked protofilament-like tubulin tetramer. *EMBO J.* **19,** 572–580 (2000).
17. Honnappa, S., Cutting, B., Jahnke, W., Seelig, J. & Steinmetz, M. O. Thermodynamics of the Op18/stathmin-tubulin interaction. *J. Biol. Chem.* **278,** 38926–38934 (2003).
18. Nogales, E., Downing, K. H., Amos, L. A. & Löwe, J. Tubulin and FtsZ form a distinct family of GTPases. *Nature Struct. Biol.* **5,** 451–458 (1998).
19. Li, H., DeRosier, D. J., Nicholson, W. V., Nogales, E. & Downing, K. H. Microtubule structure at 8 Å resolution. *Structure* **10,** 1317–1328 (2002).
20. Löwe, J. & Amos, L. A. Crystal structure of the bacterial cell-division protein FtsZ. *Nature* **391,** 203–206 (1998).
21. Müller-Reichert, T., Chrétien, D., Severin, F. & Hyman, A. A. Structural changes at microtubule ends accompanying GTP hydrolysis: Information from a slowly hydrolyzable analogue of GTP, guanylyl (α,β)methylenediphosphonate. *Proc. Natl Acad. Sci. USA* **95,** 3661–3666 (1998).
22. CCP4. The CCP4 suite: programs for protein crystallography. *Acta Crystallogr. D* **50,** 760–763 (1994).
23. Wilson, L., Bamburg, J. R., Mizel, S. B., Grisham, L. M. & Creswell, K. M. Interaction of drugs with microtubule proteins. *Fed. Proc.* **33,** 158–166 (1974).
24. Shearwin, K. E. & Timasheff, S. N. Effect of colchicine analogues on the dissociation of αβ tubulin into subunits: the locus of colchicine binding. *Biochemistry* **33,** 894–901 (1994).
25. Burns, R. G. Analysis of the colchicine-binding site of β-tubulin. *FEBS Lett.* **297,** 205–208 (1992).
26. Skoufias, D. A. & Wilson, L. Mechanism of inhibition of microtubule polymerization by colchicine: inhibitory potencies of unliganded colchicine and tubulin-colchicine complexes. *Biochemistry* **31,** 738–746 (1992).
27. Diederichs, K., McSweeney, S. & Ravelli, R. B. Zero-dose extrapolation as part of macromolecular synchrotron data reduction. *Acta Crystallogr. D* **59,** 903–909 (1992).
28. De La Fortelle, E. & Bricogne, G. in *Methods in Enzymology* (eds Carter, C. W. & Sweet, R. M.) 472–494 (Academic, New York, 1997).
29. Winn, M. D., Isupov, M. N. & Murshudov, G. N. Use of TLS parameters to model anisotropic displacements in macromolecular refinement. *Acta Crystallogr. D* **57,** 122–133 (2001).
30. Schneider, T. R. A genetic algorithm for the identification of conformationally invariant regions in protein molecules. *Acta Crystallogr. D* **58,** 195–208 (2002).

Supplementary Information accompanies the paper on **www.nature.com/nature**.

Acknowledgements We thank the ESRF for the provision of synchrotron radiation facilities. We thank E. Charbaut for discussions, C. Petosa for critical reading of the manuscript and L. Lebeau for providing us with DAMA-colchicine. This work was supported by grants from the Association pour la Recherche contre le Cancer, the CNRS and the INSERM.

Competing interests statement The authors declare that they have no competing financial interests.

Correspondence and requests for materials should be addressed to M.K. (knossow@lebs.cnrs-gif.fr). Atomic coordinates have been deposited in the Protein Data Bank under the accession codes 1SA0 (tubulin–colchicine:RB3-SLD) and 1SA1 (tubulin–podophyllotoxin:RB3-SLD).